

University of Nebraska - Lincoln
DigitalCommons@University of Nebraska - Lincoln

USGS Staff -- Published Research

US Geological Survey

2012

Hurricane disturbance and recovery of energy balance, CO₂ fluxes and canopy structure in a mangrove forest of the Florida Everglades


Jordan G. Barr
Everglades National Park

Vic Engel
Everglades National Park

Thomas J. Smith
U.S. Geological Survey

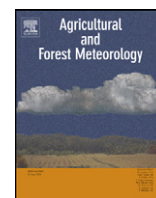
José D. Fuentes
The Pennsylvania State University, jdfuentes@psu.edu

Follow this and additional works at: <http://digitalcommons.unl.edu/usgsstaffpub>

 Part of the [Geology Commons](#), [Oceanography and Atmospheric Sciences and Meteorology Commons](#), [Other Earth Sciences Commons](#), and the [Other Environmental Sciences Commons](#)

Barr, Jordan G.; Engel, Vic; Smith, Thomas J.; and Fuentes, José D., "Hurricane disturbance and recovery of energy balance, CO₂ fluxes and canopy structure in a mangrove forest of the Florida Everglades" (2012). *USGS Staff -- Published Research*. 911.
<http://digitalcommons.unl.edu/usgsstaffpub/911>

This Article is brought to you for free and open access by the US Geological Survey at DigitalCommons@University of Nebraska - Lincoln. It has been accepted for inclusion in USGS Staff -- Published Research by an authorized administrator of DigitalCommons@University of Nebraska - Lincoln.



Hurricane disturbance and recovery of energy balance, CO₂ fluxes and canopy structure in a mangrove forest of the Florida Everglades

Jordan G. Barr^a, Vic Engel^a, Thomas J. Smith^b, José D. Fuentes^{c,*}

^a South Florida Natural Resource Center, Everglades National Park, Homestead, FL 33030, United States

^b U.S. Geological Survey, Southeast Ecological Science Center, 600 Fourth Street South, St. Petersburg, FL 33701, United States

^c Department of Meteorology, The Pennsylvania State University, University Park, PA 16802, United States

ARTICLE INFO

Article history:

Received 30 November 2010

Received in revised form 25 July 2011

Accepted 27 July 2011

Keywords:

Mangrove

Hurricane

Carbon dioxide

Energy balance

Disturbance

Sediment elevation

Carbon cycling

Sea level rise

Climate change

ABSTRACT

Eddy covariance (EC) estimates of carbon dioxide (CO₂) fluxes and energy balance are examined to investigate the functional responses of a mature mangrove forest to a disturbance generated by Hurricane Wilma on October 24, 2005 in the Florida Everglades. At the EC site, high winds from the hurricane caused nearly 100% defoliation in the upper canopy and widespread tree mortality. Soil temperatures down to –50 cm increased, and air temperature lapse rates within the forest canopy switched from statically stable to statically unstable conditions following the disturbance. Unstable conditions allowed more efficient transport of water vapor and CO₂ from the surface up to the upper canopy layer. Significant increases in latent heat fluxes (LE) and nighttime net ecosystem exchange (NEE) were also observed and sensible heat fluxes (H) as a proportion of net radiation decreased significantly in response to the disturbance. Many of these impacts persisted through much of the study period through 2009. However, local albedo and MODIS (Moderate Resolution Imaging Spectro-radiometer) data (the Enhanced Vegetation Index) indicated a substantial proportion of active leaf area recovered before the EC measurements began 1 year after the storm. Observed changes in the vertical distribution and the degree of clumping in newly emerged leaves may have affected the energy balance. Direct comparisons of daytime NEE values from before the storm and after our measurements resumed did not show substantial or consistent differences that could be attributed to the disturbance. Regression analyses on seasonal time scales were required to differentiate the storm's impact on monthly average daytime NEE from the changes caused by interannual variability in other environmental drivers. The effects of the storm were apparent on annual time scales, and CO₂ uptake remained approximately 250 g C m⁻² yr⁻¹ lower in 2009 compared to the average annual values measured in 2004–2005. Dry season CO₂ uptake was relatively more affected by the disturbance than wet season values. Complex leaf regeneration dynamics on damaged trees during ecosystem recovery are hypothesized to lead to the variable dry versus wet season impacts on daytime NEE. In contrast, nighttime CO₂ release (i.e., nighttime respiration) was consistently and significantly greater, possibly as a result of the enhanced decomposition of litter and coarse woody debris generated by the storm, and this effect was most apparent in the wet seasons compared to the dry seasons. The largest pre- and post-storm differences in NEE coincided roughly with the delayed peak in cumulative mortality of stems in 2007–2008. Across the hurricane-impacted region, cumulative tree mortality rates were also closely correlated with declines in peat surface elevation. Mangrove forest–atmosphere interactions are interpreted with respect to the damage and recovery of stand dynamics and soil accretion processes following the hurricane.

Published by Elsevier B.V.

1. Introduction

Mangrove forests are valued ecosystems due to their role in fisheries support, shoreline protection, and as a source of lumber for coastal communities. The role of these forests in global carbon

cycling is also being increasingly recognized (Bouillon et al., 2008). Mangrove forests are particularly susceptible to disturbance from tropical storms because of their location along the coast in the tropics and subtropics. During storm events, high winds, surge and sediment deposition and erosion can cause widespread defoliation, tree mortality, and changes in species composition. In extreme cases, the disturbance caused by storms can cause shifts in ecosystem type (Craighead and Gilbert, 1962; Armentano et al., 1995; Ross et al., 2001; Cahoon et al., 2003; Smith et al., 2009).

* Corresponding author.

E-mail address: jdfuentes@psu.edu (J.D. Fuentes).

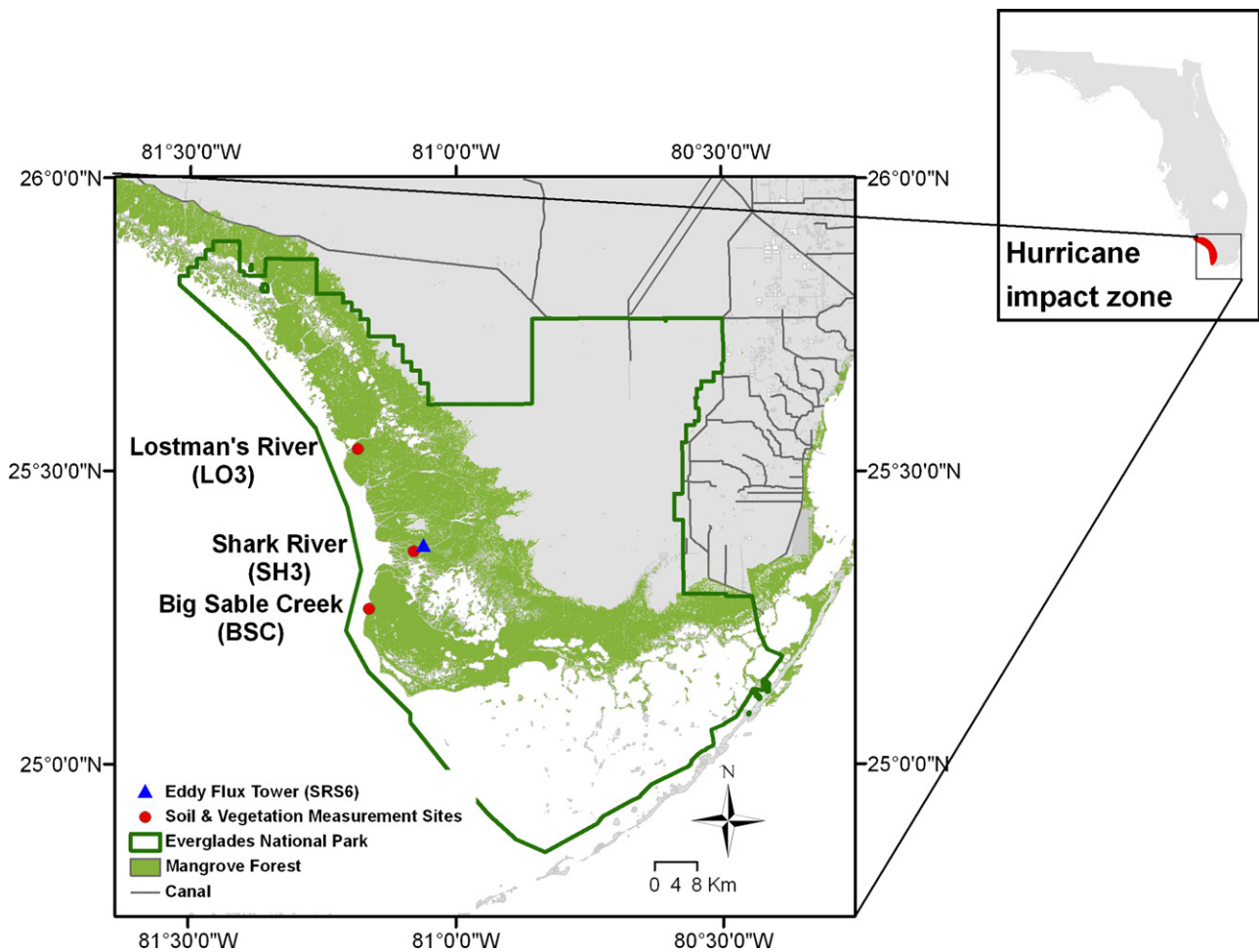


Fig. 1. Measurements to determine eddy covariance CO_2 and water vapor fluxes have taken place at the Shark River eddy flux Tower site (SRS6) in Everglades National Park since 2004. The site is located 4 km inland from the approximate center of Hurricane Wilma's landfall. Pre- and post-hurricane measurements of sediment surface elevations and forest stand structure have been recorded at Shark River (SH3), Big Sable Creek (BSC) and Lostman's River (LO3) sites. The hurricane-impacted zone is shown in red in the upper right corner (inset) of the figure. (For interpretation of the references to color in this figure legend, the reader is referred to the web version of the article.)

The recovery of mangrove canopy structure after a tropical storm comes with the production of new leaves, seedling generation, stump sprouting, and development of understory vegetation (Michener et al., 1997; Walker, 1991). The mechanisms governing the recovery of plant–soil carbon cycles, including net ecosystem CO_2 exchange (NEE), and the effects of tropical storm disturbance on ecosystem respiration are not well understood. Ellison and Farnsworth (1993) suggested that while structural damage may reduce the ability of mangrove forests to accumulate carbon over the short term, net ecosystem productivity (NEP, expressed in $\text{gCm}^{-2}\text{t}^{-1}$) over longer time periods can also be stimulated through nutrient turnover, lowered sulfide toxicity, and creation of canopy gaps. The impacts of tropical storms on mangrove forest latent (LE) and sensible (H) heat fluxes remain largely unknown.

The research questions we seek to address in this manuscript include, “How are mangrove forest and soil carbon cycles and energy balance impacted by tropical storm disturbance?”, “How do the changes in carbon and energy balance reflect the impacts to canopy structure caused by wind damage and storm surge?”, and “Over what time scales do forest carbon cycles and energy balance recover to pre-disturbance conditions?”. In order to address these questions and to assess the impacts of a tropical storm, it is necessary to account for the variability in forest carbon cycling and energy balance that is expected to occur with inter-annual variability in environmental drivers such as air temperature and salinity. Here we contrast variables such as NEE, LE, and H in a

mature mangrove forest in Everglades National Park, Florida, USA before and after Hurricane Wilma, which made landfall in this region in October 2005. Observations of tree mortality, canopy albedo, satellite-based remote sensing data, and changes in sediment elevation provide independent assessments of impact and recovery and also provide the means to relate changes in land surface–atmosphere exchanges to the hurricane impacts on canopy structure. Thus, the principal objectives of the study are to, (1) estimate changes in canopy microclimate, energy partitioning, and seasonal and annual CO_2 fluxes caused by Hurricane Wilma, and (2) relate these disturbances to the changes in canopy structure and soil dynamics during recovery from the storm. To address each of these objectives, we differentiate the expected inter-annual variability in ecosystem functioning from the changes that can be attributed to the disturbance.

2. Methods

The Barr et al. (2010) study site (SRS6; Fig. 1) was severely impacted by Hurricane Wilma, which made landfall on October 24, 2005 with sustained winds of 176 km h^{-1} . The storm defoliated much of the mangrove forest from Cape Sable to Naples, Florida and resulted in widespread mortality of trees (Smith et al., 2009). Hurricane Wilma created a natural disturbance experiment, and the resumption of EC measurements in late 2006 at the SRS6 site

provided the means to investigate several research questions relating to hurricane impacts on mangrove ecosystem functioning.

2.1. Site description

The eddy covariance (EC) tower is located at a Florida Coastal Everglades Long Term Ecological Research site (SRS6; 25.3646°N, 81.0779°W) and adjacent to a US Geological Service monitoring site (SH3) near the mouth of the Shark River, one of the principal drainages of Everglades National Park (ENP) into the Gulf of Mexico (Fig. 1). This subtropical region is characterized by distinct wet (June–October) and dry (November–May) seasons during most years. At least 60% of annual rainfall occurs during the wet season. Water levels in the coastal Everglades are relatively higher (>0.3 m) during the wet season due to increased fresh water discharge, higher rainfall, and because the peak of the annual tidal cycle also occurs during this period (Stumpf and Haines, 1998). The early part of the dry season is characterized by lower and more variable air temperatures (T_A), and periodic rain events associated with the infrequent passage of cold fronts. Annual minimum fresh-water discharge rates and annual maximum salinity values occur at the end of the dry season in April and May. Monthly values of environmental variables at the site from 2004 to 2009 are provided in Fig. 2A–D.

At the study site the dominant mangrove species include *Rhizophora mangle*, *Avicennia germinans*, and *Laguncularia racemosa*, and their maximum heights can reach 19 m. Prior to the disturbance caused by Hurricane Wilma, Chen and Twilley (1999) reported a stand density of 7450 trees ha⁻¹. The forest understory is sparse and comprised of seedlings and juvenile mangroves with an average height of less than 4 m. The region is characterized by mixed semi-diurnal tides. The site is flooded 4622 h yr⁻¹ (52% of the time) during high tides when surface water depths can reach 0.5 m (Krauss et al., 2006). Peat thickness beneath the forest increases towards the Gulf of Mexico, and at the SRS6 research site a limestone substrate lies between 5 and 6 m beneath the organic soils (Spackman et al., 1966).

Mangrove forests along the Gulf Coast of south Florida are subject to tropical storm disturbance every 3–5 years (Doyle and Girod, 1997; Hopkinson et al., 2008). Hurricane Wilma made landfall as a category 3 storm with an eye over 128-km wide centered over the SRS6 study site. The storm deposited calcitic marl from the Gulf of Mexico and Florida Bay across a 70-km zone along the western border of ENP. Between 5 and 15 cm of these deposits were found inland at a distance from 1.6 to ~5 km from the coast (Smith et al., 2009).

2.2. Meteorological, eddy covariance and energy balance measurements

Meteorological and EC measurements of NEE, LE ($W m^{-2}$), and H ($W m^{-2}$) prior to Hurricane Wilma's impact follow the methods described in Barr et al. (2010). Instruments were deployed on 30-m flux tower, which was constructed in June 2003. Environmental variables (incoming and reflected solar irradiance, net radiation, incoming and reflected photosynthetic active radiation (PAR), and wind speed and direction, air temperature, soil temperature, and soil heat fluxes) were measured at 1-s intervals and averaged over 30-min periods. Hydrologic data (water depth and specific conductivity) were recorded every 15 min at a station 30 m south of Shark River and 150 m west of the flux tower. The eddy covariance (EC) system was mounted at 27 m above the surface. The EC consists of a three-dimensional sonic anemometer (model RS-50, Gill Co., Lymington, England) and an open path infrared CO₂ and water vapor (H₂O) gas analyzer (model LI-7500, LI-COR, Inc., Lincoln, Nebraska). High-frequency (10 Hz)

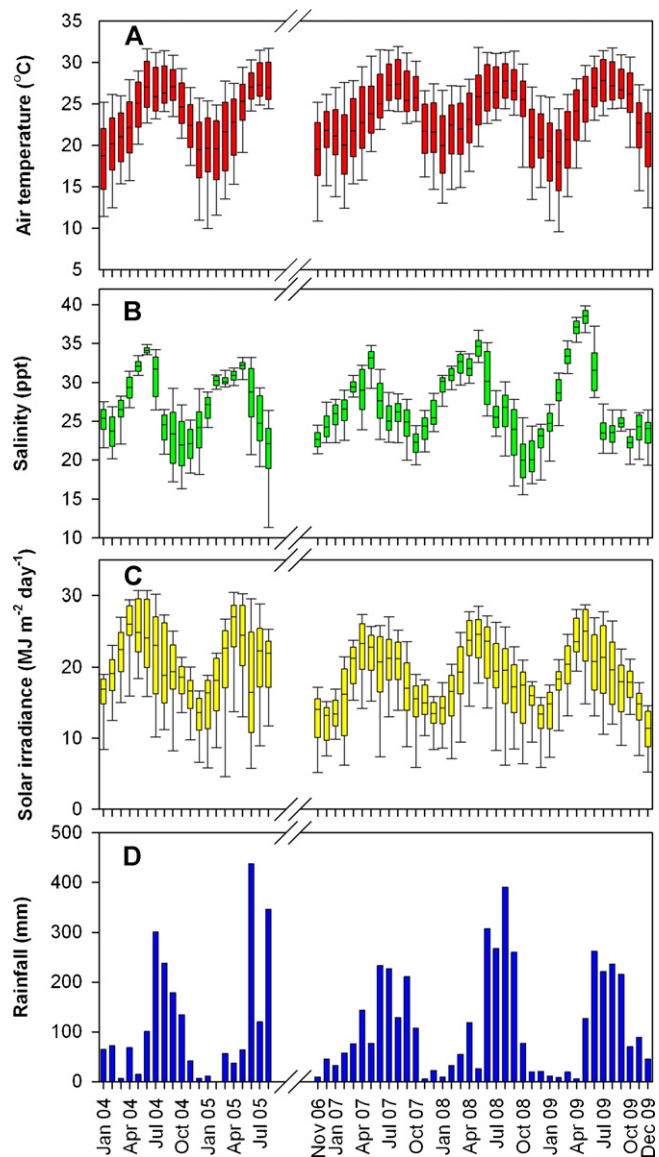


Fig. 2. (A) Monthly air temperature (°C) at a height of 27 m, (B) pore-water salinity (parts per thousand; ppt), (C) solar irradiance ($W m^{-2} day^{-1}$), and (D) total rainfall (mm) before and after Hurricane Wilma. Box plots include 25th, median (50th), and 75th percentiles of half-hourly values during the month, and whiskers indicate 5th and 95th percentiles.

measurements were recorded and processed with custom software to derive half-hourly CO₂, latent and sensible heat, and momentum exchanges between the forest and the overlying atmosphere. Spike removal from raw turbulence data was achieved using a two-dimensional coordinate rotation of the wind field (Vickers and Mahrt, 1997). Time lag corrections were made to maximize of CO₂ covariance with vertical wind speed variation. Buoyancy corrections of sonic air temperatures were also introduced (Schotanus et al., 1983). Density variations arising from water vapor were included the estimation of the total constituent flux (Webb et al., 1980). Storage of CO₂ in the air column below the EC system was estimated based on the half-hourly rate of change of CO₂ concentrations at the infrared analyzer level (e.g., Humphreys et al., 2005). The flux data included in this study are of high quality as verified from inter-comparisons with the Ameriflux algorithms (<http://public.ornl.gov/ameriflux/standards-gold.shtml>). Barr (2005) and Barr et al. (2010) provide further details about field observations and data processing.

We follow the sign convention for land surface–atmosphere scalar fluxes derived from EC data such that negative values refer to fluxes from the atmosphere to the land surface, and positive values refer to fluxes from the land surface to the atmosphere. Estimates of NEE are expressed in $\mu\text{mol}(\text{CO}_2)\text{m}^{-2}\text{s}^{-1}$, while integrated values over monthly or annual periods are given in $\text{gCm}^{-2}\text{t}^{-1}$ and represent $-\Sigma\text{NEE}$ values. Average values ± 1 standard deviation are reported separately for daytime and nighttime periods and further partitioned into dry (November–May) and wet (June–October) seasons. Hurricane Wilma destroyed the tower structure, instruments, and electronics. The site was rebuilt and the same measurements described in Barr et al. (2010) made during 2004–2005 were restarted in November 2006. Soil thermocouples were identical in positioning and model to those deployed in 2004–2005. New aspirated and shielded platinum temperature probes (model 41342VC, R.M. Young Co., Traverse City, MI) were used to measure T_A at heights of 27 m, 20 m, and 1.5 m after the storm.

2.3. Gap-filling missing data

Missing or invalid EC fluxes, referred to as ‘gaps’, occur during power failures, when gas concentrations are out-of-range as occurs during rainfall events (due to raindrops resting on the mirror of the LI-7500 instrument), when turbulence is weak or intermittent (the u^* threshold), or when there is insufficient fetch. Short duration gaps (≤ 4.5 h) in the EC data occurred primarily at night during low turbulence conditions. The u^* -threshold below which flux data were excluded (Goulden et al., 1996; Lee et al., 1999) was calculated by first dividing nighttime NEE values into 20 u^* classes for each bi-monthly period, and then defining a u^* value above which NEE became invariant. For those bi-monthly periods where no clear relationship between NEE and u^* existed, u^* values were chosen to correspond to an NEE not less than 85% of the maximum bi-monthly NEE (Barr et al., 2010). Median value of all bi-monthly u^* threshold quantities calculated before Hurricane Wilma was 0.21m s^{-1} , and varied between 0.15m s^{-1} and 0.30m s^{-1} . During three bi-monthly periods prior to Hurricane Wilma, the u^* threshold was $>0.25\text{m s}^{-1}$. However, the differences in fluxes calculated during these periods using a u^* threshold of 0.21m s^{-1} versus greater values (up to 0.3m s^{-1}) were not significant. Therefore, a global u^* -threshold of 0.21m s^{-1} was applied to all bi-monthly periods. The same u^* threshold analysis was performed on nighttime flux data from 2006 to 2009 collected after the storm. For those periods, flux calculations made during periods when u^* values were below the post-storm, bi-monthly average threshold of 0.14m s^{-1} were excluded. Flux data were also excluded when the flux footprint (Schuepp et al., 1990; Schmid, 2002) extended beyond the forest fetch. The footprint exceeded the fetch most frequently during the nighttime with wind direction from northwest to northeast.

Gaps in the dataset exceeding 4.5 h were generally caused by instrument or data acquisition malfunction. Prior to the hurricane, the combined duration of gaps comprised 61%, 28%, and 46% of the total nighttime, daytime, and combined datasets, respectively. Following the storm in 2007, gaps comprised 67%, 49%, and 58% of the total nighttime, daytime, and combined datasets, respectively. In 2008, gaps comprised 56%, 25%, and 41% of total nighttime, daytime, and combined datasets, and in 2009 gaps comprised 51%, 15%, and 34% of the nighttime, daytime, and combined datasets, respectively.

A mean diurnal variation (MDV) method was used to fill short gaps and look-up tables (LUT) were employed to fill longer gaps. The MDV method is used to fill individual gaps using the mean fluxes occurring during the same half-hourly period within a 14-day window centered on the day of the gap. For longer gaps, separate daytime and nighttime LUTs were developed for each 2-month interval beginning on January 1, 2004. Nighttime T_A was better

correlated with CO_2 fluxes than T_S and was therefore chosen as the independent variable in the LUT. For each 2-month interval, half-hourly nighttime CO_2 fluxes were partitioned into 20 T_A bins, each containing the same number of values. For daytime half-hourly CO_2 fluxes, a two-dimensional LUT was constructed using 16-PAR and 3- T_A bin categories (Falge et al., 2001). Potential error and bias in the fluxes introduced by the MDV and the LUT were estimated by randomly creating and then re-filling 100 sets of artificial gaps (Moffat et al., 2007) overlapping with valid data periods for each bi-monthly period. Barr et al. (2010) demonstrated that the root mean square error (RMSE; $3.56 \pm 0.058\ \mu\text{mol}(\text{CO}_2)\text{m}^{-2}\text{s}^{-1}$) and the bias error (BE; $-0.021 \pm 0.054\ \mu\text{mol}(\text{CO}_2)\text{m}^{-2}\text{s}^{-1}$) associated with this technique imputed minimal error in annual NEE estimates. Gap-filled, half-hourly NEE data were integrated to produce monthly and annual total values for the period January 2004 to December 2009. Gap-filled EC data were also integrated during daytime periods only to produce LE and H estimates over daily, monthly, and annual timescales. MDV and LUT methods were used to fill short (≤ 4.5 h) and long (>4.5 h) duration gaps, respectively in LE and H estimates. Only daytime gaps were filled, and the two-dimensional LUT was constructed using 16 solar irradiance bins and 3 vapor pressure deficit bins. MDV and LUT methods were also used to fill gaps in net radiation during daytime periods, and the LUT was constructed using 16 solar irradiance bins and 3 air temperature bins.

2.4. Remote sensing, stand surveys, and sediment elevations

Values of the Enhanced Vegetation Index (EVI) from the Moderate Resolution Imaging Spectro-radiometer (MODIS) aboard NASA's Terra satellite were used to examine the magnitude and duration of Hurricane Wilma's impact on canopy reflectance and light interception. EVI is particularly sensitive to the vegetation signal, resists saturation in high biomass regions, provides for de-coupling of background and vegetation signals, and reduces signals attributed to atmospheric conditions (Huete et al., 2002). EVI values were derived from the MOD13A1 data product (EOS; <http://modis.gsfc.nasa.gov/>). The EC study site is included in grid h10v06, with a 500-m spatial resolution. Using GIS (Geographic Information System) software (Matlab Mapping Toolbox, The Mathworks Inc., Natick, MA), the 16-day average EVI values for the pixel corresponding to the location of the study site and the 8 adjacent pixels were extracted for the period from 2000 to 2009. This 9-pixel domain approximates the extent of the EC measurement footprint (see Barr et al., 2010; Fig. 1). Each 16-day composite EVI value consists of up to 64 observations. However, typically fewer than 10 observations were included in a composite value after exclusion of values during cloudy and off-nadir periods. Minimum and maximum EVI values range between 0 and 1.

Surveys of tree growth and mortality, and soil elevations at three sites in the impact zone were initiated several years prior to Hurricane Wilma. The least impacted site on the Lostmans River (LO3) is located 22.1 km from the EC site (Fig. 1). The SH3 site, located 150 m from the EC tower, experienced greater impacts and approximately 100% defoliation. The Big Sable Creek (BSC) site lies 13.7 km from the EC tower and is 400 m from the Gulf of Mexico. This site experienced more exposure to wind and storm surge during Hurricane Wilma compared to the other sites. Stand surveys began at these sites following Hurricane Andrew in September 1992. Circular plots of variable radii were established in which all stems >1.5 m in height were tagged and measured for diameter at breast height (≈ 1.4 m). The first surveys following Hurricane Wilma took place in November 2005. Additional surveys of all stems >1.5 m have been carried out intermittently since the disturbance. Sediment elevation table (SET) benchmarks are located at the center of each site. Quarterly surveys of changes in soil surface elevation, with a total error of ± 1.4 mm began in March 2002 (Whelan et al.,

2005). Relative elevation changes caused by Hurricane Wilma were determined by subtracting the last elevation measurement made before the storm from all subsequent measurements.

2.5. Statistical analyses

A multivariate ridge regression model (Hoerl and Kennard, 1970) was applied to distinguish the direct effects of disturbance on monthly daytime, nighttime, and daytime plus nighttime NEE from the independent, inter-annual variation in these quantities due to non-hurricane environmental drivers. The ridge regression employs the following relationship:

$$\hat{\chi} = (A^T A + \Gamma)^{-1} A^T b \quad (1)$$

In (1), $\hat{\chi}$ is the set of regression coefficients that minimizes the sum of squared error of predictions of the response variable b (in this case monthly NEE). The coefficient matrix, A , consists of the explanatory variables indexed by columns and sequential monthly replicates indexed by rows. Explanatory variables were monthly median T_A at 27 m ($^{\circ}\text{C}$; Fig. 2A), median soil temperature T_S at -5 cm ($^{\circ}\text{C}$), monthly sum of solar irradiance (MJ m^{-2}), median surface water salinity (parts per thousand; Fig. 2B), the fraction of time the site was inundated during each month, and monthly rainfall (mm; Fig. 2D). Monthly rainfall was based on the mean value recorded at three nearby monitoring stations located at a distance of ~ 3 km, ~ 5 km, and ~ 13 km from the tower. Ordinary least squares regression (OLSR) minimizes the sum of squared errors of the predicted values. The minimization only applies to data sets used to train the model. However, when applied to new data sets, the resulting coefficients do not necessarily provide a model which minimizes the sum of squared errors. To overcome this problem, regularization (Γ) of the coefficients in the vector is performed (Hoerl and Kennard, 1970). In this procedure, Γ is defined as the product of α and the identity matrix, I (i.e., $\Gamma = \alpha I$). Typically, α is determined numerically by selecting the value that minimizes the prediction of MSE from a validation data set.

Three different models were built with the response variables of observed, monthly integrated daytime ($-\Sigma\text{NEE}_{\text{day,obs}}$), nighttime ($\Sigma\text{NEE}_{\text{nt,obs}}$), and 24-h total NEE ($-\Sigma\text{NEE}_{\text{tot,obs}}$). The final value of α in each model was selected to minimize MSE using values from 2004 to 2005. A leave-one-out (LOO) cross validation procedure (Picard and Cook, 1984) was used to compute MSE for each value of α . Data on environmental variables from the years 2006 to 2009 were applied to the NEE models to produce monthly estimates of daytime ($-\Sigma\text{NEE}_{\text{day,mod}}$), nighttime ($\Sigma\text{NEE}_{\text{nt,mod}}$), and 24-h total NEE ($-\Sigma\text{NEE}_{\text{tot,mod}}$) for post-storm periods. The differences between modeled and observed monthly NEE values provide estimates of the changes in CO_2 fluxes resulting solely from the disturbance. The average differences in modeled and measured monthly values were compared to zero using a one-sided t -test for the periods 2006–2007, 2008, and 2009. A rejection of the null hypothesis that the mean monthly pre- and post-storm difference in ΣNEE was equal to zero at the 95% confidence level was interpreted as a significant disturbance effect.

3. Results

3.1. Tree mortality and changes in canopy radiative properties

Hurricane Wilma resulted in the widespread death of trees >1.5 m in height (Fig. 3). In general, tree mortality decreased with distance from the center of landfall where the highest wind speeds occurred. At the BSC site close to the Gulf shoreline, cumulative tree mortality reached 45% in October 2007. At the SH3 site near the EC system during the first 6 months after the storm, mortality rates reached approximately 25% of the stems >1.5 m in height.

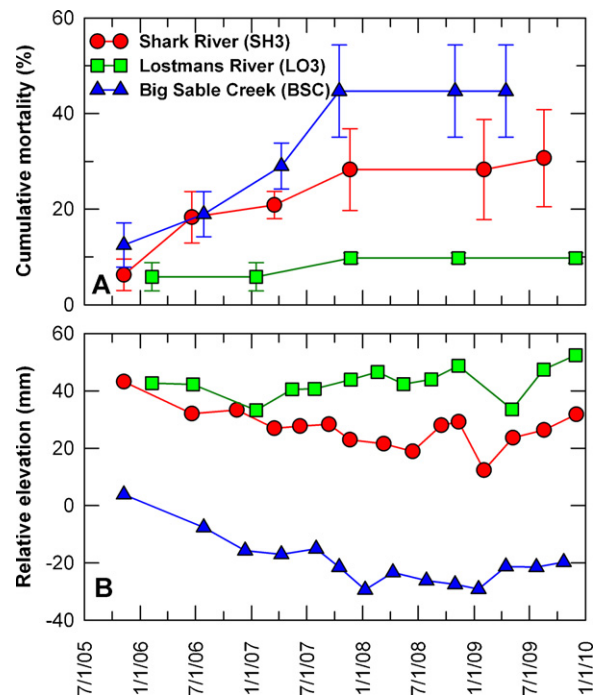


Fig. 3. Hurricane Wilma made landfall on October 24, 2005 and caused widespread and delayed mortality (A) of trees >1.5 m in height at these sites. Error bars represent ± 1 standard deviation from the mean percentage of dead to total number of stems observed in multiple plots of variable radii at each site. Sediment elevations, relative to the last measurements made before the storm in 2005 (B) declined at the SH3 and BSC sites until the beginning of 2009.

Cumulative tree mortality was lowest at the LO3 site, reaching 10% in November 2007.

MODIS EVI data provided evidence of the leaf area changes in the mangrove forest in response to the passage of Hurricane Wilma (Fig. 4). EVI values in the 9-pixel domain around the tower location immediately after the storm were reduced by approximately 50% from pre-storm values. In mid-May 2006, approximately 6 months after the storm, EVI values increased sharply with the onset of the annual wet season. However, average EVI values remained lower following the disturbance. A t -test showed a significant difference ($P < 0.001$) in the mean (\pm s.d.) 2004–2005, pre-storm (0.470 ± 0.041) and 2006–2009 post-storm (0.420 ± 0.040) EVI values derived for the 9-pixel domain. The mean (\pm s.d.) EVI values for the single pixel covering the tower location before the storm (0.446 ± 0.054) were also significantly lower after the disturbance

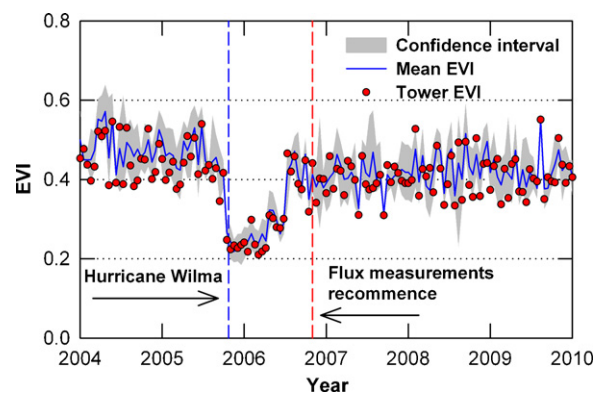


Fig. 4. Enhanced Vegetation Index (EVI) values at the tower location for pre- and post-Hurricane Wilma periods during which eddy-covariance data were also available. Confidence bands represent the minimum and maximum EVI values of the site pixel and 8 adjacent pixels during each 16-day averaging period.

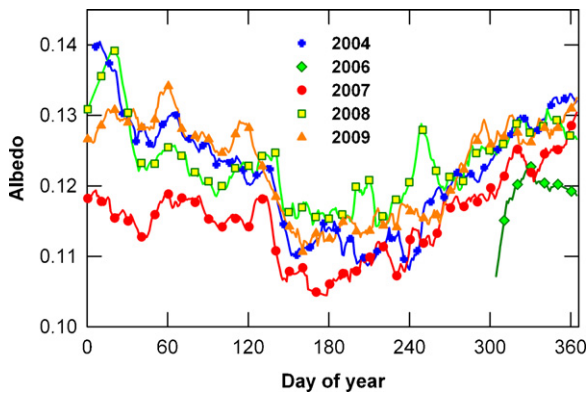


Fig. 5. Five-day moving average of mean daily (8:00–16:00 h) albedo during 2004 and 2006 through 2009.

(0.407 ± 0.049 ; $P < 0.001$). Intra-annual and inter-annual EVI values were variable and did not exhibit clear seasonal patterns before or after the storm. Both before and after the storm, the forest exhibited strong seasonal trends in albedo synchronized with summer and winter solstices (Fig. 5). On average, the surface albedo was 10% lower during the first year of measurements after Hurricane Wilma compared to pre-storm conditions. Albedo values in 2009 matched the pre-storm, 2004 observations.

3.2. Soil and air temperature profiles

With a few exceptions, significant increases ($P < 0.01$) in T_S were measured between -5 cm and -50 cm following Hurricane Wilma compared to 2004–2005 values (Table 1) during both daytime and nighttime periods. The most noteworthy exception occurred in dry season T_S values at -5 cm, which exhibited significant increases relative to pre-storm values only during 2007–2008. The inherent spatial variability in soil radiative fluxes in forests with variable amounts of coarse woody debris and litter thickness may have

independently influenced soil surface temperatures. Soil warming following the disturbance was more apparent in nighttime compared to daytime T_S values at all depths.

Some significant differences in pre- and post storm average T_A values were observed, but these were not sufficient to account for the observed increases in T_S . In the 2006–2007 dry season for example, both daytime and nighttime T_A were significantly lower, while daytime T_S values were relatively unchanged and nighttime T_S values were significantly higher compared to 2004–2005 pre-storm values. In the 2007–2008 dry season, the above-canopy T_A values recorded at 27 m and the T_S values at all depths during both daytime and nighttime periods were significantly greater than pre-storm values. However, during this period the temperature gradients between surface soil T_S and above-canopy T_A values were also significantly different compared to the temperature gradients observed before the storm due to the warmer T_S . The increases in T_S after the storm led to significantly smaller daytime and significantly larger nighttime temperature gradients between surface soil T_S and above-canopy T_A in 2006–2008.

Within-canopy air temperature lapse rates between 1.5 m and 20 m were significantly affected by Hurricane Wilma. Following the disturbance, positive lapse rates (i.e., lower T_A with height above the substrate) were observed during the dry and wet seasons of 2007 and 2008. Sensor failure prevented the calculation of lapse rates in 2009. Before the disturbance, solar heating of the intact upper canopy layers generally resulted in negative lapse rates between these two measurement heights. The positive lapse rates after the storm are indicative of increased atmospheric instability inside the forest canopy. During 2007 the bi-monthly average (± 1 s.d.) u -threshold of 0.18 ± 0.10 m s⁻¹ was 25% lower than the monthly average value found in 2004.

3.3. Solar irradiance and net radiation partitioning

Incoming mid-day solar irradiance K_{in} values were on average higher during 2004 than years 2005–2009 (data not shown). The R_{net}/K_{in} ratios (Table 2) were also generally higher following the

Table 1

Mean ± 1 s.d. of half-hourly soil temperature (T_S), air temperature (T_A), soil–air temperature differences (-5 cm to 27 m) and within-canopy lapse rates between (1.5–20 m) for dry (November to May) and wet (June to October) seasons before and after Hurricane Wilma. Similar letter superscripts in columns identify results that are not significantly different ($P > 0.01$) within each season during daytime (10:00–14:00 h) or nighttime (0:00–4:00 h) periods using a two-sided t -test with Bonferroni correction.

Year	T_{soil} (°C) (–50 cm)	T_{soil} (°C) (–20 cm)	T_{soil} (°C) (–5 cm)	T_{air} (°C) (1.5 m)	T_{air} (°C) (20 m)	T_{air} (°C) (27 m)	$[T_{soil(-5cm)} - T_{air(27m)}]$ (°C)	Lapse rate (°C km ⁻¹)
Dry season, daytime								
2004	21.1 \pm 1.9 ^a	21.0 \pm 2.4 ^a	20.7 \pm 2.8 ^a	23.5 \pm 3.6 ^b	24.3 \pm 3.4 ^{bc}	24.2 \pm 3.4 ^b	–3.5 \pm 2.1 ^a	–47 \pm 30 ^a
2004–2005	21.7 \pm 2.2 ^b	21.2 \pm 2.7 ^a	20.9 \pm 3.2 ^a	23.1 \pm 4.2 ^{ab}	23.9 \pm 3.9 ^b	23.8 \pm 3.8 ^b	–3.0 \pm 2.3 ^b	–48 \pm 44 ^a
2006–2007	22.7 \pm 1.4 ^c	21.4 \pm 2.0 ^a	21.0 \pm 2.3 ^a	22.2 \pm 3.6 ^a	21.9 \pm 3.8 ^a	21.5 \pm 3.8 ^c	–0.5 \pm 3.0 ^d	13 \pm 28 ^c
2007–2008	24.0 \pm 1.5 ^d	24.0 \pm 1.8 ^b	23.5 \pm 2.1 ^b	26.5 \pm 2.9 ^c	26.5 \pm 2.7 ^d	25.9 \pm 2.7 ^a	–2.4 \pm 2.0 ^c	–1 \pm 33 ^b
2008–2009	21.2 \pm 2.5 ^a	21.1 \pm 3.2 ^a	20.6 \pm 3.6 ^a	NA	24.5 \pm 3.8 ^c	24.1 \pm 3.7 ^b	–3.5 \pm 2.7 ^a	NA
Wet season, daytime								
2004	27.4 \pm 0.7 ^b	27.3 \pm 0.9 ^a	27.3 \pm 1.1 ^a	29.3 \pm 1.9 ^a	29.7 \pm 1.8 ^b	29.6 \pm 1.8 ^a	–2.3 \pm 1.4 ^a	–26 \pm 29 ^b
2005	26.9 \pm 0.6 ^a	27.2 \pm 0.8 ^a	27.5 \pm 1.1 ^a	29.2 \pm 2.0 ^{ab}	30.1 \pm 1.4 ^a	29.5 \pm 1.6 ^a	–2.1 \pm 1.5 ^a	–48 \pm 59 ^a
2007	28.2 \pm 1.4 ^d	28.1 \pm 1.5 ^c	27.9 \pm 1.5 ^b	29.6 \pm 2.1 ^b	29.0 \pm 2.1 ^d	29.1 \pm 2.1 ^b	–1.2 \pm 2.1 ^c	34 \pm 35 ^d
2008	27.8 \pm 0.8 ^c	27.6 \pm 1.3 ^b	27.4 \pm 1.5 ^a	29.6 \pm 2.7 ^b	29.4 \pm 2.6 ^c	29.0 \pm 2.5 ^b	–1.6 \pm 1.9 ^b	14 \pm 41 ^c
2009	28.1 \pm 0.9 ^d	28.3 \pm 0.9 ^d	28.1 \pm 1.0 ^c	NA	30.4 \pm 1.6 ^a	29.8 \pm 1.6 ^a	–1.7 \pm 1.7 ^b	NA
Dry season, nighttime								
2004	21.0 \pm 1.9 ^a	21.2 \pm 2.5 ^a	21.0 \pm 2.7 ^a	18.4 \pm 3.6 ^a	18.9 \pm 4.0 ^b	18.3 \pm 3.7 ^b	2.7 \pm 2.1 ^a	–26 \pm 38 ^a
2004–2005	21.5 \pm 2.2 ^b	21.1 \pm 2.6 ^a	20.8 \pm 2.9 ^a	18.2 \pm 3.9 ^a	18.6 \pm 4.3 ^b	18.3 \pm 4.0 ^b	2.5 \pm 2.5 ^a	–22 \pm 50 ^a
2006–2007	23.2 \pm 1.3 ^c	22.3 \pm 1.9 ^b	22.2 \pm 2.1 ^b	17.8 \pm 3.7 ^a	17.0 \pm 4.0 ^a	16.7 \pm 3.8 ^a	5.5 \pm 2.5 ^d	44 \pm 22 ^c
2007–2008	24.4 \pm 1.5 ^d	24.8 \pm 1.8 ^c	24.9 \pm 1.9 ^c	21.8 \pm 2.9 ^b	21.3 \pm 3.0 ^c	20.9 \pm 3.0 ^c	4.1 \pm 1.9 ^c	27 \pm 28 ^b
2008–2009	21.6 \pm 2.5 ^b	21.7 \pm 3.2 ^b	21.9 \pm 3.4 ^b	NA	18.9 \pm 4.2 ^b	18.6 \pm 4.1 ^b	3.3 \pm 2.3 ^b	NA
Wet season, nighttime								
2004	27.5 \pm 0.7 ^a	27.7 \pm 1.0 ^a	27.4 \pm 1.1 ^a	25.3 \pm 1.9 ^a	25.5 \pm 1.8 ^c	24.7 \pm 1.8 ^b	2.7 \pm 1.1 ^b	–9 \pm 58 ^b
2005	27.0 \pm 0.9 ^a	27.6 \pm 1.0 ^{ab}	27.3 \pm 1.2 ^{ab}	25.5 \pm 1.2 ^{ab}	26.9 \pm 1.4 ^a	26.0 \pm 1.0 ^a	1.3 \pm 1.0 ^a	–78 \pm 54 ^a
2007	28.6 \pm 1.1 ^c	28.7 \pm 1.3 ^c	28.7 \pm 1.4 ^c	26.1 \pm 1.1 ^b	25.0 \pm 1.1 ^d	25.2 \pm 1.2 ^a	3.5 \pm 1.0 ^d	59 \pm 21 ^d
2008	28.1 \pm 0.8 ^b	28.1 \pm 1.3 ^b	28.1 \pm 1.5 ^b	26.1 \pm 2.1 ^b	25.2 \pm 2.2 ^{cd}	24.9 \pm 2.1 ^{ab}	3.1 \pm 1.3 ^c	52 \pm 27 ^c
2009	28.2 \pm 1.4 ^b	28.8 \pm 1.5 ^c	28.8 \pm 1.7 ^c	NA	25.9 \pm 1.4 ^b	25.7 \pm 1.5 ^a	3.1 \pm 1.9 ^c	NA

Table 2
Mean \pm 1 s.d. of daytime (10:00–14:00 h) half-hourly sensible (H) and latent (LE) heat fluxes, ratios of net to solar irradiance (R_{net}/K_{in}), H/R_{net} , LE/R_{net} , soil heat fluxes (G), and energy closure ($(H+LE)/(R_{net}-G)$) for dry (November to May) and wet (June to October) seasons before and after Hurricane Wilma. Similar letter superscripts in columns identify results that are not significantly different ($P > 0.01$) within each season during daytime or nighttime periods using a two-sided t -test with Bonferroni correction.

Year	H ($W m^{-2}$)	LE ($W m^{-2}$)	R_{net}/K_{in}	H/R_{net}	LE/R_{net}	G ($W m^{-2}$)	$(H+LE)/(R_{net}-G)$
Dry season, daytime							
2004	195 \pm 74 ^a	197 \pm 70 ^b	0.784 \pm 0.001 ^b	0.330 \pm 0.003 ^a	0.333 \pm 0.003 ^a	16 \pm 12 ^b	0.681 \pm 0.004 ^b
2004–2005	169 \pm 86 ^b	176 \pm 73 ^a	0.777 \pm 0.001 ^a	0.325 \pm 0.003 ^b	0.339 \pm 0.003 ^b	7 \pm 11 ^a	0.673 \pm 0.004 ^a
2006–2007	137 \pm 78 ^d	230 \pm 109 ^{cd}	0.789 \pm 0.001 ^c	0.286 \pm 0.003 ^e	0.483 \pm 0.006 ^d	32 \pm 24 ^c	0.825 \pm 0.007 ^e
2007–2008	144 \pm 73 ^d	239 \pm 99 ^d	0.790 \pm 0.002 ^d	0.289 \pm 0.002 ^d	0.479 \pm 0.004 ^d	16 \pm 14 ^b	0.793 \pm 0.005 ^d
2008–2009	158 \pm 74 ^c	221 \pm 99 ^c	0.778 \pm 0.002 ^a	0.316 \pm 0.002 ^c	0.442 \pm 0.004 ^c	16 \pm 13 ^b	0.783 \pm 0.004 ^c
Wet season, daytime							
2004	149 \pm 68 ^a	265 \pm 84 ^b	0.806 \pm 0.002 ^a	0.249 \pm 0.002 ^a	0.443 \pm 0.004 ^b	9 \pm 10 ^a	0.703 \pm 0.005 ^b
2005	126 \pm 63 ^b	221 \pm 78 ^a	0.817 \pm 0.005 ^b	0.240 \pm 0.005 ^b	0.420 \pm 0.008 ^a	9 \pm 7 ^{ab}	0.670 \pm 0.011 ^a
2007	86 \pm 61 ^d	302 \pm 121 ^{cd}	0.830 \pm 0.002 ^d	0.171 \pm 0.002 ^e	0.608 \pm 0.008 ^d	12 \pm 15 ^c	0.799 \pm 0.008 ^c
2008	99 \pm 63 ^c	287 \pm 118 ^c	0.819 \pm 0.001 ^b	0.198 \pm 0.002 ^c	0.578 \pm 0.006 ^c	14 \pm 15 ^c	0.799 \pm 0.007 ^c
2009	99 \pm 60 ^c	314 \pm 116 ^d	0.823 \pm 0.001 ^c	0.195 \pm 0.002 ^d	0.623 \pm 0.006 ^e	10 \pm 12 ^b	0.835 \pm 0.006 ^d

disturbance compared to pre-storm values. However, by the dry season of 2008–2009, R_{net}/K_{in} ratios were not significantly different than 2004–2005 values.

Significant reductions in daytime sensible heat fluxes (H ; $W m^{-2}$) above the canopy were observed after the storm. For example, the average-hourly, mid-day H and H/R_{net} values were significantly lower compared to 2004–2005 values, and relatively stronger reductions were observed in the wet compared to dry season months (Table 2). In both dry and wet seasons, mid-day H and H/R_{net} values remained significantly lower than pre-disturbance values through 2009. In contrast to the results for H , dry and wet season latent heat fluxes (LE ; $W m^{-2}$) were higher after the disturbance compared to 2004–2005 values. Monthly total daytime LE and LE/R_{net} both before and after the storm were highly variable, but the seasonal average values of both variables were significantly higher through 2009 compared to pre-storm values. Applying a constant latent heat of vaporization of 43.74 kJ mol⁻¹ to these LE fluxes and taking into account seasonal variations suggests that annual evapotranspiration rates increased by as much as 25% (~ 250 mm yr⁻¹) above 2004–2005 values.

Soil heat fluxes (G ; $W m^{-2}$) also increased significantly following the hurricane. The largest increases in mid-day G were observed during the 2006–2007 dry season in the first year of measurements after the storm (Table 2). The magnitude of the dry season increases in G from 2004 to 2005 values declined with time after the disturbance, and by 2007–2008 the dry season G was not significantly different from pre-storm values. Average wet season G values returned to pre-disturbance values in 2009.

3.4. Net ecosystem exchange of CO₂

By the time the EC measurements began 1 year after Hurricane Wilma in November 2006, daytime NEE, particularly during the wet seasons following the storm, had largely recovered to pre-storm conditions. The near-complete recovery of daytime NEE is consistent with our observations of substantial regrowth of foliage in the canopy and with the comparisons of pre- and post-storm EVI values (Fig. 4). However, several key differences in pre- and post-storm NEE values were still apparent in the EC data. For example, in March 2007, the mid-day CO₂ uptake rates were reduced by 5–8 μ mol (CO₂) m⁻² s⁻¹ compared to March 2004 (Fig. 6A). These differences in NEE were not attributed to differences in the local climate, as environmental conditions above the canopy were similar during these 2 months (Fig. 6B–E). The differences observed in March 2004 and March 2007 were characteristic of the overall impacts of the storm on dry season CO₂ uptake rates. In contrast, during the 2007 wet season, the average monthly mid-day CO₂ uptake rates differed from pre-storm values by a maximum of 4 μ mol (CO₂) m⁻² s⁻¹. The average nighttime net ecosystem CO₂ exchange rates (i.e. nighttime

respiration) during wet and dry seasons following Hurricane Wilma were higher by as much as 0.5 μ mol (CO₂) m⁻² s⁻¹ and 2 μ mol (CO₂) m⁻² s⁻¹, respectively.

The impacts of Hurricane Wilma were less apparent in the seasonal comparisons of average monthly total NEE values before and after the storm. Inter-annual and intra-annual variability in the environmental factors that influence NEE tended to obscure the direct impacts of the disturbance on CO₂ fluxes. For example, standard t -tests showed the differences between the values of average monthly total daytime ($-\Sigma NEE_{day}$), nighttime (ΣNEE_{nt}) and the 24-h total net ecosystem CO₂ exchange ($-\Sigma NEE_{tot}$) observed in both dry and wet seasons before and after the storm were insignificant (Table 3). Similar results were obtained using the non-parametric Mann–Whitney–Wilcoxon rank-sum test. The most consistent differences in pre- and post-storm average monthly values were found in wet season nighttime respiration (ΣNEE_{nt}) values. Pre- and post-storm monthly ΣNEE values (including daytime, nighttime, and 24-h total values) showed the most divergence in 2007–2008, possibly due to the delayed peak in mortality of stems which occurred during this period. The general lack of consistent and significant pre- and post-storm differences in dry season, wet season or annual ΣNEE may be partly attributed to the relatively small sample sizes ($n = 7, 5,$ or 12) within each group, and to

Table 3

Mean \pm 1 s.d. monthly total net ecosystem CO₂ exchanges during daytime ($-\Sigma NEE_{day}$) nighttime (ΣNEE_{nt}), and daytime plus nighttime 24-h CO₂ exchange ($-\Sigma NEE_{tot}$) for dry (November to May) and wet (June to October) seasons before and after Hurricane Wilma. Similar letter superscripts in columns identify results that are not significantly different ($P > 0.05$) within each season using a two-sided t -test with Bonferroni correction.

Year	$-\Sigma NEE_{day}$ ($g C m^{-2}$)	ΣNEE_{nt} ($g C m^{-2}$)	$-\Sigma NEE_{tot}$ ($g C m^{-2}$)
Dry season			
2004	158 \pm 26 ^a	46 \pm 7 ^{a,b}	113 \pm 23 ^a
2004–2005	146 \pm 18 ^a	45 \pm 6 ^a	101 \pm 23 ^a
2006–2007	128 \pm 29 ^a	57 \pm 11 ^{a,b}	72 \pm 31 ^{a,b}
2007–2008	126 \pm 13 ^a	61 \pm 9 ^b	65 \pm 19 ^b
2008–2009	133 \pm 23 ^a	51 \pm 9 ^{a,b}	81 \pm 23 ^{a,b}
Wet season			
2004	151 \pm 7 ^a	65 \pm 14 ^{a,b}	87 \pm 14 ^{a,b}
2005	148 \pm 11 ^a	49 \pm 3 ^a	100 \pm 6 ^a
2007	149 \pm 17 ^a	77 \pm 5 ^b	72 \pm 22 ^{a,b}
2008	136 \pm 11 ^a	71 \pm 5 ^b	64 \pm 11 ^b
2009	144 \pm 5 ^a	70 \pm 10 ^{a,b}	74 \pm 13 ^{a,b}
Dry and wet seasons			
2004	154 \pm 19 ^a	55 \pm 14 ^{a,b}	100 \pm 22 ^a
2004–2005	146 \pm 16 ^{a,b}	46 \pm 6 ^a	101 \pm 19 ^a
2006–2007	137 \pm 26 ^{a,b}	65 \pm 14 ^b	72 \pm 26 ^{a,b}
2007–2008	130 \pm 13 ^b	65 \pm 9 ^b	65 \pm 16 ^b
2008–2009	137 \pm 18 ^{a,b}	59 \pm 13 ^{a,b}	78 \pm 19 ^{a,b}

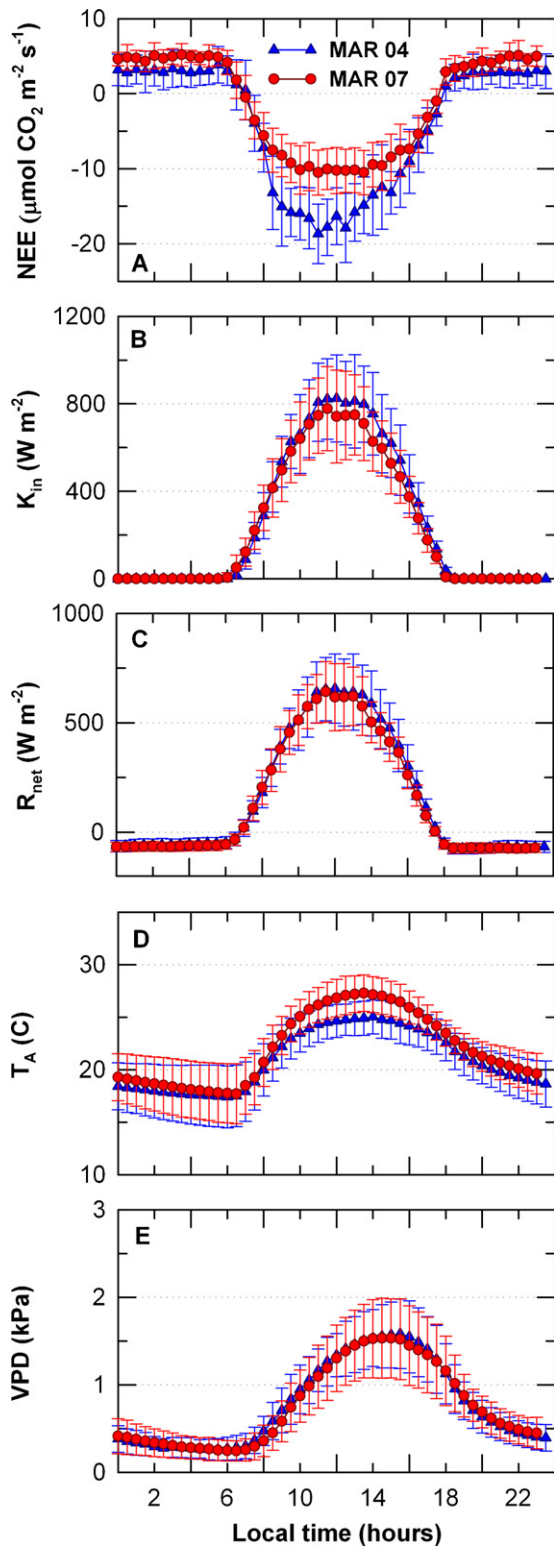


Fig. 6. Mean diurnal NEE trends (A) show net daytime CO₂ uptake was lower in March 2007 (after Hurricane Wilma) compared to March 2004. Differences in NEE were attributed to the storm disturbance but not to differences in environmental variables including K_{in} (B), R_{net} (C), and T_A (D) and VPD (E). Error bars represent ± 1 standard deviation around the mean half-hourly values.

the magnitude of variability in ΣNEE compared to mean monthly values.

Visual comparisons of the time series of monthly $-\Sigma NEE_{day}$, ΣNEE_{nt} and $-\Sigma NEE_{tot}$ values before and after the storm showed distinct but variable disturbance impacts. Consistent differences

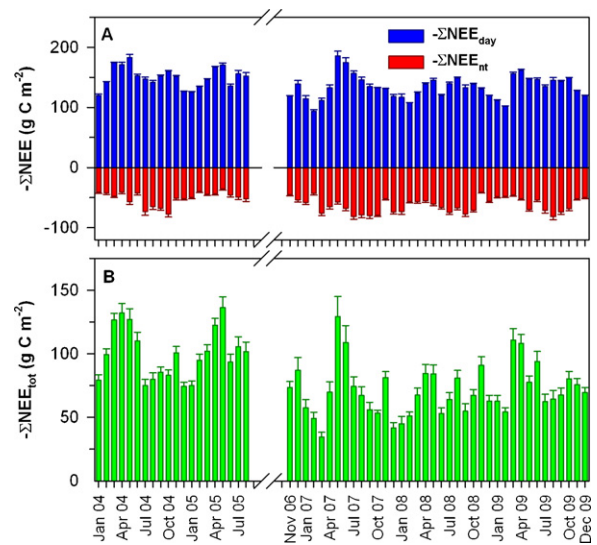


Fig. 7. Monthly integrated (A) daytime ($-\Sigma NEE_{day}$) and nighttime (ΣNEE_{nt}), and (B) 24-h total ($-\Sigma NEE_{tot}$) net ecosystem CO₂ exchange.

in pre- and post-storm monthly $-\Sigma NEE_{day}$ were generally not apparent, and exhibited similar seasonal variation before and after Hurricane Wilma (Fig. 7A). Maximum uptake rates occurred in the late dry season both before and after the storm. In two distinct periods after the storm (May–June 2007 and in March–April 2009), sharp increases in daytime CO₂ uptake rates above the wintertime minima were observed which matched or exceeded the corresponding values before the storm. The effects of storm were more apparent in the pre- and post-storm ΣNEE_{nt} and $-\Sigma NEE_{tot}$ comparisons. Post-storm ΣNEE_{nt} values (Fig. 7A) were consistently higher (i.e., greater total nighttime respiratory CO₂ fluxes), and as a result, the 24-h total CO₂ uptake ($-\Sigma NEE_{tot}$) values were consistently lower (Fig. 7B). The variability in $-\Sigma NEE_{tot}$ values also increased after the storm.

f-Tests showed the ridge regression model (Eq. (1)) accurately predicted $-\Sigma NEE_{day}$, ΣNEE_{nt} , and $-\Sigma NEE_{tot}$ for 2004–2005 ($P < 0.001$ for each predictand). Comparisons between the modeled and observed monthly integrated daytime ($-\Sigma NEE_{day}$), nighttime (ΣNEE_{nt}), and 24-hr total CO₂ exchange ($-\Sigma NEE_{tot}$) for post-hurricane periods confirmed our observations that the relative magnitude of the storm’s impact on CO₂ exchange depended partly on the season. In this scheme, the average differences between modeled and observed ΣNEE values that were significantly greater or less than zero indicated a disturbance effect that was independent of the effect of other environmental drivers. We found our assessment of the storm’s impact on daytime ΣNEE depended on the length of time over which the average differences in modeled and observed values were determined. For example, the modeled, average monthly total daytime CO₂ uptake ($-\Sigma NEE_{day,mod}$) values were often greater than observed values ($-\Sigma NEE_{day,obs}$; Fig. 8A) but the magnitudes of these differences were not consistent across seasons (Table 4) and they did not decline over time as might be expected in a recovering system. The average difference between $-\Sigma NEE_{day,mod}$ and $-\Sigma NEE_{day,obs}$ determined seasonally was significantly different from zero ($P < 0.01$) only for the 2007–2008 dry season. The differences in $-\Sigma NEE_{day,mod}$ and $-\Sigma NEE_{day,obs}$ for the wet seasons of 2007–2009 were not significantly different from zero. However, the average differences between $-\Sigma NEE_{day,mod}$ and $-\Sigma NEE_{day,obs}$ determined on an annual basis ($n = 12$) were significantly greater than zero in 2007–2008 and 2008–2009, but not in 2006–2007. This suggests the lack of consistent, significant differences in $-\Sigma NEE_{day,mod}$ and $-\Sigma NEE_{day,obs}$ for the dry seasons following the storm may have been due in part to the small sample

Table 4
Mean \pm 1 s.d. of the differences between modeled (Eq. (1)) and observed monthly total daytime net CO₂ exchange $-(\Sigma NEE_{\text{day,mod}} - \Sigma NEE_{\text{day,obs}})$, nighttime net CO₂ exchange $(\Sigma NEE_{\text{nt,mod}} - \Sigma NEE_{\text{nt,obs}})$, and net daytime plus nighttime 24-h CO₂ exchange $-(\Sigma NEE_{\text{tot,mod}} - \Sigma NEE_{\text{tot,obs}})$ after Hurricane Wilma. *P*-values were determined by comparing mean differences in modeled and measured values to zero using a one-sided *t*-test.

Period	Number of months	$-(\Sigma NEE_{\text{day,mod}} - \Sigma NEE_{\text{day,obs}})$ (g C m ⁻² month ⁻¹)	<i>P</i>	$\Sigma NEE_{\text{nt,mod}} - \Sigma NEE_{\text{nt,obs}}$ (g C m ⁻² month ⁻¹)	<i>P</i>	$-(\Sigma NEE_{\text{tot,mod}} - \Sigma NEE_{\text{tot,obs}})$ (g C m ⁻² month ⁻¹)	<i>P</i>
Dry season							
2006–2007	7	12 \pm 24	0.24	3 \pm 14	0.64	23 \pm 29	0.08
2007–2008	7	16 \pm 6	<0.01	-8 \pm 7	0.03	34 \pm 12	<0.01
2008–2009	7	10 \pm 14	0.10	-8 \pm 13	0.13	21 \pm 17	0.02
2006–2009	21	13 \pm 16	<0.01	-4 \pm 12	0.11	26 \pm 20	<0.01
Wet season							
2007	5	0 \pm 17	0.96	-21 \pm 4	<0.01	27 \pm 20	0.04
2008	5	9 \pm 14	0.24	-19 \pm 6	<0.01	32 \pm 13	<0.01
2009	5	6 \pm 10	0.28	-21 \pm 6	<0.01	28 \pm 12	0.01
2007–09	15	5 \pm 14	0.20	-20 \pm 5	<0.01	29 \pm 14	<0.01
Dry and wet seasons							
2006–2007	12	7 \pm 22	0.29	-7 \pm 16	0.15	25 \pm 25	0.01
2007–2008	12	13 \pm 11	<0.01	-12 \pm 9	<0.01	33 \pm 12	<0.01
2008–2009	12	8 \pm 12	0.04	-14 \pm 12	<0.01	24 \pm 15	<0.01
2006–2009	36	9 \pm 15	<0.01	-11 \pm 13	<0.01	27 \pm 18	<0.01

sizes ($n=7$) combined with high interannual variability in other environmental drivers. When grouped across years (2006–2009), the average differences between $-\Sigma NEE_{\text{day,mod}}$ and $-\Sigma NEE_{\text{day,obs}}$ revealed a significant hurricane effect on the dry season ($P<0.01$) but not wet season ($P=0.20$) daytime CO₂ uptake rates. The magnitude of the changes in monthly $-\Sigma NEE_{\text{day}}$ relative to pre-storm values was also generally greater in the dry seasons than the wet seasons.

Modeled values of monthly total nighttime respiratory CO₂ fluxes ($\Sigma NEE_{\text{nt,mod}}$) consistently underestimated observations (Fig. 8B), and unlike the results for daytime CO₂ fluxes, the largest differences occurred during the wet rather than the dry seasons after the storm. For example, the values for $\Sigma NEE_{\text{nt,mod}} - \Sigma NEE_{\text{nt,obs}}$ were significantly different from zero ($P<0.01$) during all the wet seasons through 2009. On the other hand, dry season values of $\Sigma NEE_{\text{nt,mod}} - \Sigma NEE_{\text{nt,obs}}$ were significantly different from zero ($P=0.03$) only during 2007–2008. Similarly, the average difference between seasonal $\Sigma NEE_{\text{nt,mod}}$ and $\Sigma NEE_{\text{nt,obs}}$ pairs grouped across years (2006–2009) revealed a significant hurricane impact on wet season ($P<0.01$) but not dry season ($P=0.11$) nighttime respiration rates.

Grouping the dry and wet season values showed the average differences between modeled and observed daytime and nighttime CO₂ fluxes were significant ($P<0.04$) in all years with the exception of 2006–2007. The apparent lack of a distinct hurricane impact on 2006–2007 CO₂ fluxes in the first year of our measurements may have been due to the delayed mortality of stems observed across the impact zone and at the EC site. Modeled values of monthly integrated, total 24-h CO₂ fluxes ($-\Sigma NEE_{\text{tot,mod}}$) significantly overestimated observations (Fig. 8C) during all periods with the exception of the 2006–2007 dry season ($P=0.08$).

The impacts of Hurricane Wilma were most apparent in the comparisons of annual CO₂ uptake rates before and after the storm. Annual total CO₂ uptake in the first year of measurements following the storm exhibited an approximate 30% reduction compared to average annual uptake rates in 2004–2005 (Table 5). In 2008, annual CO₂ uptake rates were again approximately 30% lower compared to 2004–2005 values and in 2009, the annual CO₂ uptake rates were 21% lower than pre-storm values.

3.5. Discussion

3.5.1. Changes in canopy radiative properties and energy balance

Field observations of the impact zone immediately after Hurricane Wilma revealed substantial and widespread defoliation as

well as significant numbers of downed stems and large branches (Smith et al., 2009). Estimates of mortality of stems caused by the storm (Fig. 3) are comparable to mortality rates measured as a result of insect outbreaks and severe fires in other forests (Amiro et al., 2010). Although measurements of the changes in leaf area in the forest before and after the storm were not available, the distinct reductions in EVI (Fig. 4) and albedo (Fig. 5) after the storm confirmed the severity of the impact on the forest. EVI decreases as light absorption through photosynthesis decreases (Huete et al., 2002), and the decreases in surface albedo following the storm may have been due to a greater proportion of solar radiation being absorbed by surface water and the moist dark soils beneath the damaged canopy. Both EVI and the albedo data indicated that the most severe effects of Hurricane Wilma occurred within the first year following the disturbance prior to the resumption of our EC measurements, but the two measures produced different estimates for the total duration of the storm's impact. The EVI data suggest the effects of the storm persisted through 2009, while the albedo data suggest recovery in canopy radiative properties was complete by mid-2008. The discrepancy may be due to spatially variable impacts of the storm and to the different measurement areas and sensitivity of these two indices.

We suggest the differences in EC and energy balance data before and after Hurricane Wilma through at least mid-2008 can be attributed to several linked mechanisms originating from wind damage to the canopy. First, we ascribe the decreases in the u_* threshold to changes in canopy roughness caused by the loss of large limbs and the toppling of stems. Gu et al. (2005) also showed the u_* threshold can change over time and space depending on the leaf area index, stem density, and canopy height. Second, we suggest the reductions in biomass and light interception in the upper

Table 5

Annual total ($\pm 90\%$ C.I.) of daytime-only ($-\Sigma NEE_{\text{day}}$), nighttime-only (ΣNEE_{nt}), and daytime plus nighttime 24-h ($-\Sigma NEE_{\text{tot}}$) net ecosystem CO₂ exchange.

Year	$-\Sigma NEE_{\text{day}}$ (g C m ⁻²)	ΣNEE_{nt} (g C m ⁻²)	$-\Sigma NEE_{\text{tot}}$ (g C m ⁻²)
2004	1821 \pm 30	656 \pm 41	1172 \pm 64
2005 ^a	1753 \pm 32	575 \pm 34	1176 \pm 66
2007	1631 \pm 49	810 \pm 44	823 \pm 84
2008	1562 \pm 28	752 \pm 38	806 \pm 66
2009	1644 \pm 21	713 \pm 34	926 \pm 70

^a January–August 2005 data collected before Hurricane Wilma. Annual 2005 values were calculated by multiplying September–December 2004 ΣNEE values by the ratio of January–August 2005 ΣNEE to January–August 2004 ΣNEE and adding the result to January–August 2005 ΣNEE .

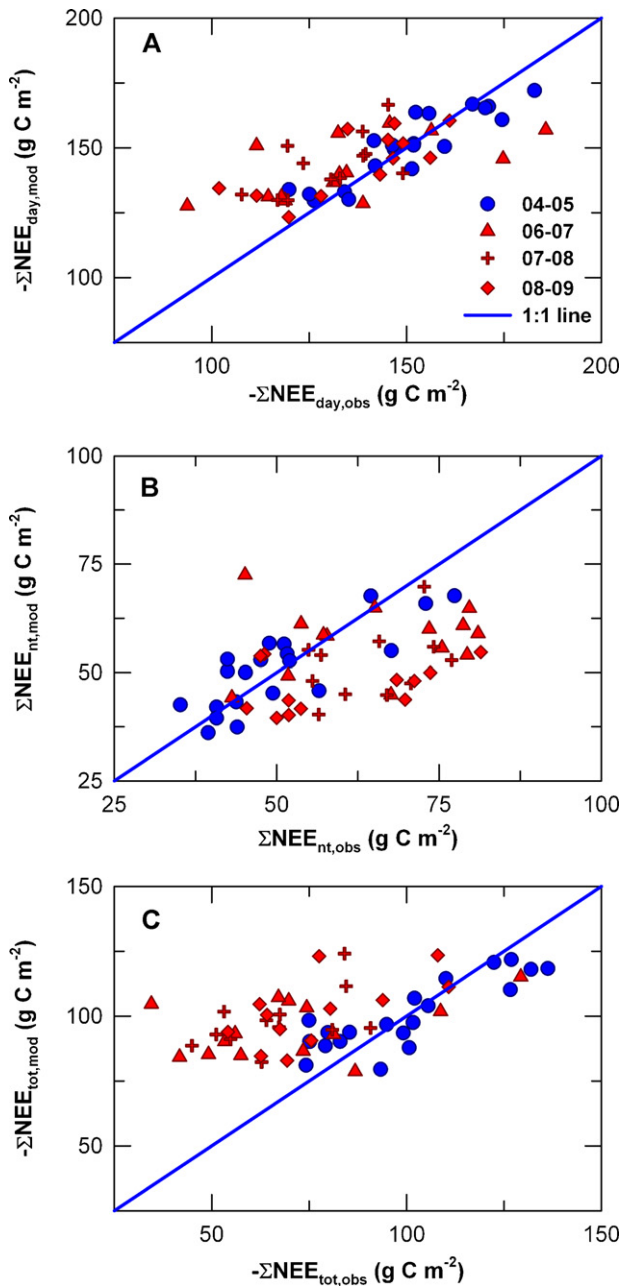


Fig. 8. Comparison of ridge-regression model estimates versus observed, monthly integrated (A) daytime ($-\Sigma NEE_{\text{day}}$), (B) nighttime (ΣNEE_{nt}), and (C) 24-h total ($-\Sigma NEE_{\text{tot}}$) net ecosystem CO₂ exchange during January 2004 to August 2005 (04–05), and the three, 12-month (November–October) hydrologic years following disturbance.

canopy led to decreases in both the radiative fluxes from the upper canopy to the atmosphere and to the significant decreases observed in H (Table 2). The reduction in heating in the upper canopy layers would also have contributed to the observed shift from predominately negative to positive lapse rates between 1.5 and 20 m, and in the shift from statically stable to statically unstable conditions within the canopy. These lapse rates contributed to more efficient mixing of air masses between the lower and upper-canopy layers and the atmosphere. Lastly, we also suggest that the relatively higher soil temperatures and higher soil heat fluxes after the storm (Table 1) may have been the result of the increased penetration of solar irradiance through the damaged canopy. In turn, the greater amount of available energy in the lower canopy appears to have enhanced direct evaporation from the open water and saturated

soil surfaces. In support of this hypothesis we note that after the storm, LE/R_{net} ratios increased by up to 40%, while H/R_{net} ratios decreased by 10–30% (Table 2). The pre- and post-storm differences in the partitioning of available energy into LE and H declined between 2006 and 2009 as the canopy recovered towards the pre-disturbance state.

Following the storm, the percent closure of the surface energy budget ($(H+LE)/(R_{\text{net}}-G)$) during the daytime improved from 67–70% to 79–83% during 2004–2005 and 2006–2009, respectively (Table 2). This degree of closure is within the range of values reported for FluxNet sites across 50-site years (Wilson et al., 2002) and boreal forests (Barr et al., 2006; Sanchez et al., 2010). For the mangrove forest, one potential cause of the surface energy imbalance includes the lateral transport of heat associated with high and low tides. Studies in other tidally influenced ecosystems (e.g., salt marshes) have reported daytime energy closure as low as 49% (e.g. Moffett et al., 2010).

3.5.2. Impacts on daytime and nighttime NEE

The ridge-regression modeling indicates that the inter-annual variability in non-hurricane drivers of NEE, such as T_A , K_{in} , and salinity (Barr et al., 2010) was not sufficient to explain the full range of post-storm differences we observed in daytime and nighttime NEE, particularly when these differences were calculated across years (Table 4, Fig. 8). However, in contrast to the soil temperature and energy balance data that suggest the impacts of Hurricane Wilma persisted until 2008, the EC measurements show that the values for average monthly total daytime NEE ($-\Sigma NEE_{\text{day}}$) after Hurricane Wilma at times approximated pre-disturbance values by late 2006 and early 2007. This was particularly evident in the comparisons of pre- and post-storm wet season daytime CO₂ uptake rates. During the first year after the storm, we observed widespread emergence of new leaves on clumped, epicormic shoots on both *L. racemosa* and *A. germinans* beneath the damaged upper canopy. Over time, branch elongation and leaf re-growth in the upper canopy occurred along with a gradual loss of leaves in the lower canopy layers, possibly as a result of light competition. These observations match with those reported following Hurricane Andrew in 1992 (Baldwin et al., 2001; Doyle et al., 1995). We speculate that the initial rapid recovery of leaf area, especially on the epicormic shoots and surviving juveniles in the lower canopy layers resulted in the relatively quick recovery of total CO₂ uptake capacity in this forest. This matches with the rapid recovery in EVI and may also explain why we did not find significant differences in average monthly $-\Sigma NEE_{\text{day}}$ during the first dry season measurements in 2006–2007. Our results also suggest that the impact of the storm on energy balance and soil temperatures persisted through the initial leaf-out and subsequent changes in leaf area distribution into 2008–2009. The relatively rapid recovery of daytime CO₂ uptake after Hurricane Wilma reflects an adaptation to the frequent disturbance from hurricanes and lightning damage in the Florida Everglades region (Smith et al., 1994; Zhang et al., 2008).

Some other aspects of canopy recovery from this disturbance also likely had an influence on our EC data. For example, using airborne LIDAR measurements, Zhang et al. (2008) showed that Hurricane Wilma, and to a lesser extent Hurricane Katrina, caused 8-fold increases in both canopy gap density and total gap area from 1.1% to 12.1% along the Shark River. Hurricane Wilma also created new gaps (roughly 10–100 m²) in the canopy immediately surrounding the EC site. Since the disturbance, substantial re-growth has occurred in such gaps, including the growth of juvenile trees that survived the storm and widespread emergence of new propagules. Variable disturbance responses among the dominant species at this site were also noted and may have influenced NEE values. *R. mangle*, one of the three co-dominant species at the EC site, does not regenerate if the plumular apex is lost or severely damaged as

often occurs during disturbance events (Gill and Tomlinson, 1971; Tomlinson, 1986). Crowns from the other two dominant species at the site, *L. racemosa* and *A. germinans*, are capable of regenerating from meristem tissue (Snedaker et al., 1992). After the initial impact from Hurricane Wilma, damaged *R. mangle* trees continued to produce leaves on surviving branches even though mortality in these trees continued to rise (Fig. 3).

In the mangrove stands of south Florida, leaf production rates are lower during the dry season (Gill and Tomlinson, 1971; Arreola-Lizárraga et al., 2004; Parkinson et al., 1999). In addition, leaf longevity increases with time after a hurricane disturbance (Ross et al., 2001). The combination of low leaf production rates in the dry season plus reductions in the average life-span of emerging leaves may have been partly responsible for the relatively stronger impact of the storm on dry season compared to wet season CO₂ uptake rates. We note that the impacts of the storm on albedo were also relatively stronger in the dry seasons compared to the wet seasons of 2007 and 2008. The largest differences in pre- and post-storm $-\Sigma\text{NEE}_{\text{day}}$ were observed in the dry season of 2007–2008, and this coincided with the peak in cumulative tree mortality after the storm at the nearby SH3 site. However, we do not fully understand why the impacts of Hurricane Wilma seemed to more conspicuously affect dry season compared to wet season CO₂ uptake rates.

The significant and persistent increase in nighttime respiratory CO₂ fluxes ($\Sigma\text{NEE}_{\text{nt}}$) was the most evident effect of Hurricane Wilma on forest–atmosphere exchanges. Several factors likely contributed to the increases in $\Sigma\text{NEE}_{\text{nt}}$, such as the decomposition of storm-generated litter and coarse woody debris (CWD). The statically unstable conditions which characterized the canopy air mass after the disturbance (Table 1) also facilitated the transport of respiratory CO₂ fluxes from soil, litter, and woody debris substrates to the EC system. Smith et al. (1994) estimated that hurricane Andrew in 1992 contributed 141 Mg ha⁻¹ of CWD in the mangrove forests on the southwest coast of Florida. Turnover times of the labile fraction of mangrove CWD in Florida range from 4 months to 23 years, and represent 10–20% of CWD by dry weight (Romero et al., 2005). Decomposition rates of the refractory components of CWD are two orders of magnitude smaller than those of the labile fraction (Romero et al., 2005) and likely contributed little to the observed increases in nighttime respiration at the tower site.

In contrast to the results for daytime CO₂ fluxes, our observations and the model results show the impact of Hurricane Wilma on nighttime CO₂ fluxes was generally larger in the wet seasons than in the dry seasons. The reason behind this trend is uncertain, though higher T_A and higher T_S during the wet seasons may have resulted in a relative increase in decomposition rates of litter and CWD generated by the storm. Across seasons, the EC data suggest the long-term effect of hurricanes on mangrove forest–atmosphere exchanges of CO₂ is manifest largely through their impact on ecosystem respiration (Table 5). The impact of hurricanes on the fluxes of particulate and dissolved inorganic and organic carbon in tidal mangrove forests should also be investigated further. The fluxes of dissolved and particulate carbon are considered to be significant components of the carbon balance in these systems (see Bouillon et al., 2008; Barr et al., 2009).

3.5.3. Soil surface elevations and ecosystem trajectories

The storm surge associated with Hurricane Wilma added approximately 43 mm of sediment elevation at SH3 and LO3 (Fig. 3B) through deposition of calcitic material. At the SH3 site, the sediment deposition was followed by a more than 20 mm decline in soil surface elevation in a span of 3 years after the storm. In a shorter-term study using SET measurements at SH3 before and after Hurricane Wilma, Whelan et al. (2009) found that the initial loss of 10.5 mm in substrate elevation at this site 6 months after the storm could be attributed to –4.9 mm of erosion in the surface

layer, –6.3 mm loss due to compaction in shallow and middle soil layers where roots are found, and a +0.8 mm expansion in the deep soil zone. Between 6 and 12 months following the storm, Whelan et al. (2009) report that erosion slowed (–3.6 mm), and the shallow soil zone expanded (6.8 mm) at SH3 as new rootlets stabilized the soil matrix and invaded the calcitic deposits. At the LO3 site, little or no elevation loss occurred during the 2 years following the storm. The trees at LO3 were defoliated during the storm but suffered much less structural damage and mortality compared to the SH3 and BSC coastal margin sites (Smith et al., 2009). The combined data from the LO3, BSC, and LO3 sites through 2009 showed that the progressive decline in soil elevation following the storm was strongly correlated ($R^2 = 0.72$) to the magnitude of cumulative tree mortality. This relationship leads to the hypothesis that root death and decomposition followed by soil compaction continued to be a primary mechanism in the loss of soil elevation after the storm. The loss of soil surface elevations in the damaged portions of this forest slowed substantially in 2009 and coincided with a leveling of cumulative mortality rates in stems. It is not known what role erosion played in the decline in soil surfaces after the storm.

The loss of sediment elevation following tree mortality at the SH3 site is concurrent with higher nighttime respiration rates measured at the nearby EC site, leading us to further hypothesize that enhanced soil carbon loss due to elevated T_S may have also contributed to the decline in soil mass (and elevation) observed at SH3 and BSC sites following the storm. Our observations show that the timing of the recovery in ecosystem respiration rates and soil temperatures to near pre-storm values in 2009 coincides with the period when declining soil surface elevations and tree mortality rates also stabilized, and this is considered as support for this hypothesis. However, since soil temperatures increased by 1–2 °C following the storm, it is likely that any increases in soil CO₂ flux caused by the higher T_S represented a relatively small fraction of the total increase in ecosystem respiration observed after the storm (Lovelock, 2008).

Despite the subsequent loss of soil surface elevations following the storm, the calcitic deposits brought by the Hurricane Wilma storm surge resulted in net gains in soil surface elevations in inland areas of the mangrove forest. However, in the areas located closest to the coast, such as those represented by the BSC site where the storm caused significant erosion, sediment elevations remained lower than pre-storm conditions. Surveys of aerial photographs from the early 1900s showed that similar hurricane impacts in the Everglades coastline resulted in permanent transitions from mangrove forests to intertidal mudflats along tidal channels draining to the Gulf of Mexico (Smith et al., 2009). Our findings also agree with the findings of Cahoon et al. (2003) who found Honduran mangrove forests that suffered partial mortality after Hurricane Mitch (1998) gained elevation with root production while the basin mangrove forests that suffered total mortality experienced irreversible peat collapse.

3.5.4. Summary and conclusions

This study produced new information to quantify the impacts of tropical storm disturbance on carbon cycling and energy balance in the mangrove forests of the Florida Everglades. The tropical storm disturbance caused structural changes in the forest that resulted in nearly 100% defoliation in the upper canopy and widespread tree mortality. Immediately after the storm, surface radiative attributes such as EVI declined by 50% compared to pre-storm values. One year after the disturbance, surface albedo remained 10% lower than before the storm. The changes in canopy architecture and leaf area after the storm appear to have allowed for greater solar irradiance transfer to the lower canopy layers and to the substrate. As a result of this disturbance, significant increases in both daytime and particularly nighttime soil temperatures down to –50 cm were

observed. Within-canopy conditions also changed from statically stable to statically unstable which contributed to efficient transport of water vapor and CO₂ from the substrate and lower canopy to the upper canopy layers. These changes contributed to greater partitioning of the available energy into latent heat fluxes and a decrease in sensible heat fluxes. Annual evapotranspiration rates were 25% higher after the storm. The pre- and post-hurricane differences in the partitioning of available energy into latent and sensible heat fluxes declined over time as the ecosystem structure approached its undisturbed state in 2009.

The most evident impact of Hurricane Wilma was observed in the persistent increase in nighttime ecosystem respiration, possibly due to decomposition of the new litter and coarse woody debris generated by the storm. Increases in belowground respiration due to the higher soil temperatures may also have contributed to higher rates of respiratory CO₂ fluxes measured after the storm. The effects on nighttime respiration were most pronounced in the wet seasons. In contrast, the damage from the storm had a more pronounced effect on CO₂ uptake during the dry seasons compared to the wet seasons. However, because much of the recovery in active leaf area occurred prior to the resumption of our EC measurements, we were often unable to consistently differentiate the independent effects of the storm from non-hurricane drivers of CO₂ uptake on seasonal time scales. This may have been due to the delay in maximum tree mortality after the storm and to complex leaf regeneration patterns on surviving stems and juveniles. The impact of the storm on annual CO₂ uptake rates was more apparent, and net carbon assimilation rates remained approximately 250 g C m⁻² yr⁻¹ lower in 2009 compared to the average annual values determined for 2004–2005.

Across the hurricane-impacted region, cumulative tree mortality rates were correlated with declines in peat surface elevation. In the most-disturbed zones, soil surface elevations remain substantially lower 4 years after the storm. Less-impacted stands exhibited a high degree of resilience and rapid recovery following Hurricane Wilma and the net sediment deposition caused by the storm may help to maintain the viability of the forests in these areas in this era of sea level rise. These new results confirm previous work in the Florida Everglades that show tropical storm disturbance is a primary factor regulating plant–soil carbon cycles and mangrove ecosystem trajectories in this region.

Acknowledgements

Dan Childers, Jay Zieman, Kevin Kotun, Gordon Anderson, Karen Balentine, James Kathilankal, Kendra Dowell, Dane Barr, and Daniel Sarmiento provided logistical support to complete the studies reported in this manuscript. Caryl Alarcon at ENP provided assistance with GIS software. Everglades National Park provided support under the Critical Ecosystem Studies Initiative (H5284-05-0020). The National Science Foundation, through the Florida Coast Everglades Long-term Ecological Research Program (DEB-9910514), and the National Institute for Climate Change Research (DE-FC02-06ER64298) also provided support for this research. The United States Geological Survey Priority Ecosystem Studies (PES) and the Comprehensive Everglades Restoration Monitoring and Assessment Plan (MAP) under Contract # IA-W912EP-03 from the US Army Corps of Engineers provided support to T. Smith.

References

- Amiro, B.D., Barr, A.G., Barr, J.G., Black, T.A., Bracho, R., Brown, M., Chen, J., Clark, K.L., Davis, K.J., Desai, A.R., Dore, S., Engel, V., Fuentes, J.D., Goldstein, A.H., Goulden, M.L., Kolb, T.E., Lavigne, M.B., Law, B.E., Margolis, H.A., Martin, T., McCaughey, J.H., Misson, L., Montes-Helu, M., Noormets, A., Randerson, J.T., Starr, G., Xiao, J., 2010. Ecosystem carbon dioxide fluxes after disturbance in forests in North America. *J. Geophys. Res. Biogeosci.*, doi:10.1029/2010JG001390.
- Armentano, T.V., Doren, R.F., Platt, W.J., Mullins, T., 1995. Effects of Hurricane Andrew on coastal and interior forests of Southern Florida: overview and synthesis. *J. Coastal Res.* SI 21, 111–144.
- Arreola-Lizárraga, J.A., Flores-Verdugo, F.J., Ortega-Rubio, A., 2004. Structure and litter fall of an arid mangrove stand on the Gulf of California, Mexico. *Aquat. Bot.* 79, 137–143.
- Baldwin, A., Egnatovich, M., Ford, M., Platt, W., 2001. Regeneration in fringe mangrove forests damaged by hurricane Andrew. *Plant Ecol.* 157, 149–162.
- Barr, J.G., 2005. Carbon sequestration by riverine mangroves in the Florida Everglades, Ph.D. dissertation, University of Virginia, Charlottesville, Virginia, 183pp.
- Barr, A.G., Morgenstern, K., Black, T.A., McCaughey, J.H., Nesci, Z., 2006. Surface energy balance closure by the eddy-covariance method above three boreal forest stands and implications for the measurement of the CO₂ flux. *Agric. For. Meteorol.* 140, 322–337.
- Barr, J.G., Fuentes, J.D., Engel, V., Zieman, J.C., 2009. Physiological responses of red mangroves to the climate in the Florida Everglades. *J. Geophys. Res. Biogeosci.* 114, G02008, doi:10.1029/2008JG000843.
- Barr, J.G., Engel, V.C., Fuentes, J.D., Zieman, J.C., O'Halloran, T.L., Smith III, T.J., Anderson, G.H., 2010. Controls on mangrove forest-atmosphere carbon dioxide exchanges in western Everglades National Park. *J. Geophys. Res. Biogeosci.*, doi:10.1029/2009JG001186.
- Bouillon, S., Borges, A.V., Castaneda-Moya, E., Diele, K., Dittmar, T., Duke, N.C., Kristensen, E., Lee, S.Y., Marchand, C., Middelburg, J.J., Rivera-Monroy, V.H., Smith III, T.J., Twilley, R.R., 2008. Mangrove production and carbon sinks: a revision of global budget estimates. *Global Biogeochem. Cycles* 22, GB2013, doi:10.1029/2007GB003052.
- Cahoon, D.R., Hensel, P., Rybczyk, J., McKee, K.L., Proffitt, C.E., Perez, B.C., 2003. Mass tree mortality leads to mangrove peat collapse at Bay Islands, Honduras after Hurricane Mitch. *J. Ecol.* 91, 1093–1105.
- Chen, R., Twilley, R.R., 1999. Patterns of mangrove forest structure and soil nutrient dynamics along the Shark River Estuary, Florida. *Estuaries* 22, 955–970.
- Craighead, F.C., Gilbert, V.C., 1962. The effects of Hurricane Donna on the vegetation of southern Florida. *Quart. J. Florida Acad. Sci.* 25, 1–28.
- Doyle, T.W., Girod, G., 1997. The frequency and intensity of Atlantic hurricanes and their influence on the structure of south Florida mangrove communities. In: Diaz, H., Pulwarty, R. (Eds.), *Hurricanes, Climate Change and Socioeconomic Impacts: A Current Perspective*. Westview Press, New York, NY, pp. 111–128.
- Doyle, T.W., Smith III, T.J., Robblee, M.B., 1995. Wind damage effects of Hurricane Andrew on mangrove communities along the southwest coast of Florida, USA. *J. Coastal Res.* SI 21, 159–168.
- Ellison, A.M., Farnsworth, E.J., 1993. Seedling survivorship, growth, and response to disturbance in Belizean mangal. *Am. J. Bot.* 80, 1137–1145.
- Falge, E., Baldocchi, D., Olson, R., Anthoni, P., Aubinet, M., Bernhofer, C., Burba, G., Ceulemans, R., Clement, R., Dolmani, H., Granier, A., Gross, P., Grünwald, T., Hollinger, D., Jensen, N.-O., Katul, G., Keronen, P., Kowalski, A., Lai, C.T., Law, B.E., Meyers, T., Moncrieff, J., Moors, E., Munger, J.W., Pilegaard, K., Rannik, Ü., Rebmann, C., Suyker, A., Tenhunen, J., Tu, K., Verma, S., Vesala, T., Wilson, K., Wofsy, S., 2001. Gap filling strategies for defensible annual sums of net ecosystem exchange. *Agric. For. Meteorol.* 107, 43–69.
- Gill, A.M., Tomlinson, P.B., 1971. Studies on the growth of red mangrove (*Rhizophora mangle*). Phenology of the shoot. *Biotropica* 3, 109–124.
- Goulden, M.L., Munger, J.W., Fan, S.M., Daube, B.C., Wofsy, S.C., 1996. Exchange of carbon dioxide by a deciduous forest: response to interannual climate variability. *Science* 271, 1576–1578.
- Gu, L., Falge, E.M., Boden, T., Baldocchi, D.D., Black, T.A., Saleska, S.R., Suni, T., Verma, S.B., Vesala, T., Wofsy, S.C., Xu, L., 2005. Objective threshold determination for nighttime eddy flux filtering. *Agric. For. Meteorol.* 128, 179–197.
- Hoerl, A.E., Kennard, R.W., 1970. Ridge regression: biased estimation for nonorthogonal problems. *Technometrics* 12, 55–67.
- Hopkinson, C.S., Lugo, A.E., Alber, M., Covich, A.P., Van Bloom, S.J., 2008. Forecasting effects of sea level rise and windstorms on coastal and inland ecosystems. *Front. Ecol. Environ.* 6, 255–263, doi:10.1890/070153.
- Huete, A., Didan, K., Miura, T., Rodriguez, E.P., Gao, X., Ferreira, L.G., 2002. Overview of the radiometric and biophysical performance of the MODIS vegetation indices. *Remote Sens. Environ.* 83, 195–213.
- Humphreys, E.R., Black, T.A., Morgenstern, K., Li, Z., Nesci, Z., 2005. Net ecosystem production of a Douglas-fir stand for 3 years following clearcut harvesting. *Global Change Biol.* 11, 450–464.
- Krauss, K.W., Doyle, T.W., Twilley, R.R., Rivera-Monroy, V.H., Sullivan, J.K., 2006. Evaluating the relative contributions of hydroperiod and soil fertility on growth of south Florida mangroves. *Hydrobiologia* 569, 311–324.
- Lee, X., Fuentes, J.D., Staebler, R.M., Neumann, H.H., 1999. Long-term observation of the atmospheric exchange of CO₂ with a temperate deciduous forest in southern Ontario, Canada. *J. Geophys. Res.* 104, 15975–15984.
- Lovelock, C.E., 2008. Soil respiration and belowground carbon allocation in mangrove forests. *Ecosystems* 11, 342–354.
- Michener, W.K., Blood, E.R., Bildstein, K.L., Brinson, M.M., Gardner, L.R., 1997. Climate change, hurricanes and tropical storms, and rising sea level in coastal wetlands. *Ecol. Appl.* 7, 770–801.
- Moffat, A.M., Papale, D., Reichstein, M., Hollinger, D.Y., Richardson, A.D., Barr, A.G., Beckstein, C., Braswell, B.H., Churkina, G., Desai, A.R., Falge, E., Gove, J.H., Heimann, M., Hui, D., Jarvis, A.J., Kattge, J., Noormets, A., Stauch, V.J., 2007. Comprehensive comparison of gap-filling techniques for eddy covariance net carbon fluxes. *Agric. For. Meteorol.* 147, 209–232.
- Moffett, K.B., Wolf, A., Berry, J.A., Gorelick, S.M., 2010. Salt marsh-atmosphere exchange of energy, water vapor, and carbon dioxide: effects of tidal

- flooding and biophysical controls. *Water Resour. Res.* 46, W10525, doi:10.1029/2009WR009041.
- Parkinson, R.W., Perez-Bedmar, M., Santangelo, J.A., 1999. Red mangrove (*Rhizophora mangle* L.) litter fall response to selective pruning (Indian River Lagoon, Florida, U.S.A.). *Hydrobiologia* 413, 63–76.
- Picard, R.R., Cook, R.D., 1984. Cross-validation of regression models. *J. Am. Stat. Assoc.* 79, 575–583.
- Romero, L.M., Smith III, T.J., Fourqurean, J.W., 2005. Changes in mass and nutrient content of wood during decomposition in a south Florida mangrove forest. *J. Ecol.* 93, 618–631.
- Ross, M.S., Ruiz, P.L., Telesnicki, G.J., Meeder, J.F., 2001. Estimating above ground biomass and production in mangrove communities of Biscayne National Park, Florida (U.S.A.). *Wetlands Ecol. Manage.* 9, 27–37.
- Sanchez, J.M., Caselles, V., Rubio, E.M., 2010. Analysis of the energy balance closure over a FLUXNET boreal forest in Finland. *Hydrol. Earth Syst. Sci.* 14, 1487–1497.
- Schmid, H.P., 2002. Footprint modeling for vegetation atmosphere exchange studies: a review and perspective. *Agric. For. Meteorol.* 113, 159–183.
- Schotanus, P., Nieuwstadt, F.T.M., De Bruin, H.A.R., 1983. Temperature measurement with a sonic anemometer and its application to heat and moisture fluctuations. *Boundary-Layer Meteorol.* 26, 81–93.
- Schuepp, P.H., LeClerc, M.Y., MacPherson, J.I., Desjardins, R.L., 1990. Footprint prediction of scalar fluxes from analytical solutions of the diffusion equation. *Boundary-Layer Meteorol.* 50, 355–373.
- Smith III, T.J., Robblee, M.B., Wanless, H.R., Doyle, T.W., 1994. Mangroves, hurricanes, and lightning strikes. *Bioscience* 44, 256–262.
- Smith III, T.J., Anderson, G.H., Balentine, K., Tiling, G., Ward, G.A., Whelan, K.R.T., 2009. Cumulative impacts of hurricanes on Florida mangrove ecosystems: sediment deposition, storm surges and vegetation. *Wetlands* 29, 24–34.
- Snedaker, S.C., Brown, M.S., Lahmann, E.J., Araujo, R.J., 1992. Recovery of a mixed-species mangrove forest in south Florida following canopy removal. *J. Coastal Res.* 8, 919–925.
- Spackman, W., Dolsen, C.P., Riegel, W., 1966. Phytogetic organic sediments and sedimentary environments in the Everglades–mangrove complex. Part I – evidence of a transgressing sea and its effect on environments of the Shark River area of southwest Florida. *Palaeontographica B* 17, 135–152.
- Stumpf, R.P., Haines, J.W., 1998. Variations in tidal level in the Gulf of Mexico and implications for tidal wetlands. *Estuarine Coastal Shelf Sci.* 46, 165–173.
- Tomlinson, P.B., 1986. *The Botany of Mangroves*. Cambridge University Press, Cambridge, UK.
- Vickers, D., Mahrt, L., 1997. Quality control and flux sampling problems for tower and aircraft data. *J. Atmos. Oceanic Technol.* 14 (3), 512–526.
- Walker, L.R., 1991. Tree damage and recovery from hurricane Hugo in Luquillo Experimental Forest, Puerto Rico. *Biotropica* 23, 379–385.
- Webb, E.K., Pearman, G.I., Leuning, R., 1980. Correction of the flux measurements for density effects due to heat and water vapor transfer. *Quart. J. Roy. Meteorol. Soc.* 106, 85–100.
- Whelan, K.R.T., Smith III, T.J., Cahoon, D.R., Lynch, J.C., Anderson, G.H., 2005. Ground-water control of mangrove surface elevation: shrink and swell varies with soil depth. *Estuaries* 28, 833–843.
- Whelan, K.R.T., Smith III, T.J., Anderson, G.H., Ouellette, M.L., 2009. Hurricane Wilma's impact on overall soil elevation and zones within the soil profile in a mangrove forest. *Wetlands* 29, 16–23.
- Wilson, K., Goldstein, A., Falge, E., Aubinet, M., Baldocchi, D., Berbigier, P., Bernhofer, C., Ceulemans, R., Dolman, H., Field, C., Grelle, A., Ibrom, A., Law, B.E., Kowalski, A., Meyers, T., Moncrieff, J., Monson, R., Oechel, W., Tenhunen, J., Valentini, R., Verma, S., 2002. Energy balance closure at FLUXNET sites. *Agric. For. Meteorol.* 113, 223–243.
- Zhang, K., Simard, M., Ross, M., Rivera-Monroy, V.H., Houle, P., Ruiz, P., Twilley, R.R., Whelan, K.R.T., 2008. Airborne laser scanning quantification of disturbances from hurricanes and lightning strikes to mangrove forests in Everglades National Park, USA. *Sensors* 8, 2262–2292.